### RESEARCH ARTICLE





# Spatiotemporal distribution of glia in and around the developing mouse optic tract

<sup>2</sup>Department of Neurobiology, Harvard Medical School, Boston, Massachusetts
<sup>3</sup>Department of Pathology and Cell Biology, College of Physicians and Surgeons, Columbia University, New York, New York
<sup>4</sup>Department of Genetics and Development, College of Physicians and Surgeons, Columbia University, New York, New York
<sup>5</sup>Department of Ophthalmology, College of Physicians and Surgeons, Columbia University, New York, New York

### Correspondence

Carol A. Mason, Columbia University, Jerome L. Greene Science Center, 3227 Broadway, Quad 3C Room L3-048—MC 9833, New York, NY 10027 Email: cam4@columbia.edu

#### **Funding information**

National Eye Institute, Grant/Award Numbers: R01 EY012736, T32 EY013933 and P30 EY019007; National Institute of General Medical Sciences R01 GM105775

### **Abstract**

In the developing mouse optic tract, retinal ganglion cell (RGC) axon position is organized by topography and laterality (i.e., eye-specific or ipsi- and contralateral segregation). Our lab previously showed that ipsilaterally projecting RGCs are segregated to the lateral aspect of the developing optic tract and found that ipsilateral axons self-fasciculate to a greater extent than contralaterally projecting RGC axons in vitro. However, the full complement of axon-intrinsic and -extrinsic factors mediating eye-specific segregation in the tract remain poorly understood. Glia, which are known to express several guidance cues in the visual system and regulate the navigation of ipsilateral and contralateral RGC axons at the optic chiasm, are natural candidates for contributing to eye-specific pre-target axon organization. Here, we investigate the spatiotemporal expression patterns of both putative astrocytes (Aldh1l1+ cells) and microglia (lba1+ cells) in the embryonic and neonatal optic tract. We quantified the localization of ipsilateral RGC axons to the lateral two-thirds of the optic tract and analyzed glia position and distribution relative to eyespecific axon organization. While our results indicate that glial segregation patterns do not strictly align with eye-specific RGC axon segregation in the tract, we identify distinct spatiotemporal organization of both Aldh1l1+ cells and microglia in and around the developing optic tract. These findings inform future research into molecular mechanisms of glial involvement in RGC axon growth and organization in the developing retinogeniculate pathway.

### KEYWORDS

astrocyte, axon, axon guidance, development, glia, microglia, retinal ganglion cell, RRID:A-11122, RRID:AB\_2224402, RRID:AB\_2491179, RRID:AB\_2556542, RRID:AB\_531793, RRID: SCR\_001775, RRID:SCR\_002285, RRID:SCR\_015807, visual system

### 1 | INTRODUCTION

Once considered mere support cells of the brain, glia are increasingly recognized for their numerous roles in neural development and function, including in neuronal migration, axon guidance, synaptic refinement, and regulation of synaptic number and function (Clarke & Barres, 2013; Lemke, 2001; Stogsdill & Eroglu, 2017). This understanding of glial function during brain development stems in part from a foundation of detailed morphological observations made by developmental neurobiologists in prior decades. The late Vivien Casagrande and her mentor, the

glial organization, morphology, and relationships with growing axons in the developing visual system (Guillery & Walsh, 1987; Hutchins & Casagrande, 1988, 1990), somatosensory cortex, and hippocampus (Hutchins & Casagrande, 1989). These studies suggested that glia contribute to the development of brain cytoarchitecture, including the well-defined layers within the dorsal lateral geniculate nucleus (dLGN), the thalamic target of retinal axons (Hutchins & Casagrande, 1988), and paved the way for more recent focus on glial contribution to synaptic development and refinement in the dLGN (e.g., Chung et al., 2013; Schafer et al., 2012).

late Ray Guillery used meticulous light and electron microscopy to detail

The visual system, in particular the retinogeniculate pathway, is a long-standing model for studying axon guidance and neural circuit

M.A.L. and A.A.S. contributed equally to this paper.

508

© 2018 Wiley Periodicals, Inc. wileyonlinelibrary.com/journal/cne J Comp Neurol. 2019;527:508–521.

<sup>&</sup>lt;sup>1</sup>Department of Neuroscience, Columbia University's Mortimer B. Zuckerman Mind Brain Behavior Institute, New York, New York

509

formation (reviewed in Herrera, Erskine, & Morenilla-Palao, 2017). In the binocular vertebrate visual system, RGC axons exit the retina and extend through the optic nerve to the optic chiasm at the midline, a complex intermediate choice point for growing axons, where some RGC axons cross the midline to project contralaterally and others turn away from the chiasm region to project ipsilaterally (reviewed in Petros, Rebsam, & Mason, 2008). After navigating the decussation choice at the chiasm, RGC axons extend through the optic tract to innervate the dLGN and the superior colliculus (SC), the vision-processing targets in the thalamus.

As appreciation for the diversity of glial contributions to brain development increased (reviewed in Barres & Barde, 2000), researchers continued to utilize the visual system to study glial function in neural development and plasticity. Much of the exploration of glia in the developing visual system centered on the optic nerve, chiasm (Mason & Sretavan, 1997), and the dLGN (e.g., Hutchins & Casagrande, 1988, 1990). Light and electron microscopic analyses in fish and mammals revealed frequent contact between RGC axons in the optic nerve, with interfascicular glia extending processes alongside axons (Bovolenta & Mason, 1987; Guillery & Walsh, 1987; Maggs & Scholes, 1986; Williams & Rakic, 1985). Notably, the orientation of glia changes between the nerve and chiasm, which in turn corresponds to changes in RGC growth cone morphology. In the nerve, glia are interfascicular, growing with the direction of extending axons (Maggs & Scholes, 1986), which have tapered, torpedo-like growth cones, indicating relatively guick and unhindered growth (Bovolenta & Mason, 1987; Godement, Wang, & Mason, 1994; Mason & Wang, 1997).

In the chiasm, glia extend radially from the ventral aspect of the midline of the nascent diencephalon rather than interfascicular among axons, creating a glial palisade through which RGC axons are guided to their ipsilateral or contralateral trajectory (reviewed in Mason & Sretavan, 1997). Detailed morphological studies showing increased ramification and slower extension of growth cones navigating through the optic chiasm radial glia (Bovolenta & Mason, 1987; Godement et al., 1994; Guillery & Walsh, 1987; Maggs & Scholes, 1986; Mason & Wang, 1997; Reese, Maynard, & Hocking, 1994) suggested that the glia provide selective guidance cues to ipsi- and contralateral RGC axons. Indeed, subsequent molecular studies have revealed some of these cues (e.g., Kuwajima et al., 2012; S. E. Williams et al., 2003). While midline radial glia in the chiasm are critical for the successful navigation of ipsi- and contralateral RGC axons to the appropriate side of the brain, little is known about glia in the optic tract. Of the few studies that directly examined glia in the optic tract, most were not performed in mouse (e.g., Inoue, 1970; Levine, 1989; Reese, Johnson, Hocking, & Bolles, 1997; Vanselow, Thanos, Godement, Henke-Fahle, & Bonhoeffer, 1989), and those performed in mouse were only able to draw limited conclusions on the presence and morphology, but not distribution, of glia in the tract (Colello & Guillery, 1992).

To address the gap in our knowledge of glia in the murine retinogeniculate pathway, we used classic anatomical approaches, in a similar vein to Vivien Casagrande's work (Hutchins & Casagrande, 1988, 1989), to assess glia in the embryonic and neonatal mouse optic tract. Specifically, we examined the distribution of putative astrocytes and

microglia in the context of pre-target organization of ipsilateral and contralateral RGC axons in the tract. Pre-target axon organization, a common feature of axon tracts (e.g., Imai et al., 2009; Zhou et al., 2013), is likely mediated by intrinsic axon–axon interactions, which are important for axon targeting (Wang et al., 2014), and extrinsic factors, including cues from surrounding cells, such as glia in and around the tract. RGC axons in the developing mouse retinogeniculate pathway are organized by both topography (Chan & Chung, 1999) and laterality (i.e., ipsi- and contralateral axons; Godement, Salaun, & Imbert, 1984), and ipsilateral RGC axons self-fasciculate more than contralateral axons *in vitro* (Sitko, Kuwajima, & Mason, 2018). However, other mechanisms mediating pre-target axon order in the developing optic tract, in particular, the tendency of ipsilateral RGC axons to course in the lateral tract, remain poorly understood.

Therefore, we used genetic labeling of ipsilateral RGC axons and putative astrocytes and antibody labeling of radial glia and microglia to detail glia number, distribution, and morphology along the mediolateral and rostrocaudal axes of the developing optic tract. While there is no apparent glial segregation paralleling that of ipsi- and contralateral RGC axons, we find distinct spatiotemporal organization of putative astrocytes and microglia within the tract and along the outer walls of the tract. The results presented here open the door to future studies examining the molecular identity of optic tract glia and how they might interact with axons to guide pre-target axon organization and/or early axon targeting decisions as they exit the tract to innervate their targets.

### 2 | MATERIALS AND METHODS

### 2.1 | Animals

Mice were maintained in a timed-pregnancy colony in a barrier facility at Columbia University Medical Center. All procedures were carried out in compliance with protocols approved by Columbia University's Institutional Animal Care and Use Committee. Breeding female mice were checked for vaginal plug midday each weekday. The day of plug detection was considered embryonic day (E) 0, and embryos were harvested from dams as close to midday on the day of collection as possible. ET33 SERT-Cre and Aldh1l1-eGFP mice were generated by GENSAT (Gong et al., 2007), and E33-SERT-Cre::ZsGreen mice were provided as a gift from Dr. Tom Maniatis (Columbia University). Aldh1l1-eGFP mice were obtained as a gift from the Dr. Ben Barres (Stanford University). All mice were maintained on a C57BL/6J background.

### 2.2 | Immunohistochemistry

Embryos were harvested from pregnant dams anesthetized with ketamine/xylazine (100 and 10 mg/kg, respectively, in 0.9% saline). Postnatal day (P) 0 mice were anesthetized with ketamine/xylazine (100 and 10 mg/kg, respectively, in 0.9% saline). E16, E18, and P0 mice were transcardially perfused with 4% paraformaldehyde (PFA), and E14 mice were drop-fixed after harvest and decapitation without being perfused. Brains were post-fixed in 4% PFA at 4°C overnight, followed by

TABLE 1 Antibodies used in experiments

	Antigen	Immunogen	Manufacturer, species, mono- or polyclonal, catalog or lot no., RRID	Dilution used
Primary antibodies	ZsGreen	Recombinant full-length <i>Zoanthus</i> sp. Green fluorescent protein (ZsGreen)	Clontech, rabbit polyclonal, Cat. #632474, Lot #1508409; RRID: AB _2491179	1:500
	GFP	GFP isolated directly from the jellyfish Aequorea victoria	Thermo Fisher, rabbit, Cat. #A-11122, Lot #1891900; RRID: A-11122	1:500
	lba1	Synthetic peptide corresponding to Human Iba1 aa 135-147 (C terminal)	Abcam, goat polyclonal, Cat. #ab5076, RRID: AB 2224402	1:100
	Neurofilament	Membrane preparations from rat E14-E15, recognizes 165kD protein	Developmental Studies Hybridoma Bank (DSHB), deposited by Dr. Tom Jessell and Dr. Jane Dodd, mouse monoclonal IgG, Clone 2H3, RRID: AB_531793	1:5
	RC2 (Nestin)	Fetal brain lysate from rat E14-E15, recognizes 295kD protein	Developmental Studies Hybridoma Bank (DSHB), deposited by Dr. Miyuki Yamamoto, mouse monoclonal MlgM, Clone RC2, RRID: AB_531887	1:5
Secondary antibodies	Anti-rabbit IgG Alexa Fluor 488		Thermo Fisher, donkey, Cat. #R37114, RRID: AB_2556542	1:400
	Anti-goat IgG Alexa Fluor 594		Thermo Fisher, donkey, Cat. #A-11058, RRID: AB_2534105	1:400
	Anti-mouse IgG Alexa Fluor 647		Thermo Fisher, donkey, Cat. #A-31571, RRID: AB_162542	1:400
	Anti-mouse IgM Alexa Fluor 647		Thermo Fisher, goat, Cat. # A-21238, RRID: AB_2535807	1:400

immersion in a 10% sucrose-PBS solution, then 30% sucrose-PBS at  $4^{\circ}\text{C}$  for 48 hr each or until the tissue no longer floated. After sucrose equilibration, brains were embedded in OCT and frozen on dry ice for cryosectioning.

SERT-Cre::ZsGreen and Aldh1I1-eGFP brains were cryosectioned 25  $\mu m$  thick and collected serially onto four sets of slides. One set of slides was immunostained for each experiment, resulting in sections 100  $\mu m$  apart. Slides were washed for 5 min three times with  $1\times$  PBS and blocked in 10% Normal Donkey Serum (NDS) in  $1\times$  PBS with 0.25% Tween (PBST) at room temperature (RT) for 1 hr. Slides were then incubated in primary antibody mix overnight and washed for 5 min three times with  $1\times$  PBS, followed by a 2 hr RT incubation in secondary antibody mix, then a 10 min RT incubation in 1:1000 Hoechst:PBST solution. After a final set of three 5 min washes of PBS at RT, slides were coverslipped with Fluoro-Gel mounting medium. See below for antibodies used, and Table 1 for antibody concentrations and details.

For examination of radial glia and Aldh1l1+ cell colocalization, cryosections of Aldh1l1-eGFP brains were stained with a primary antibody mix composed of 5% NDS in  $1\times$  PBST, rabbit anti-GFP, and mouse anti-RC2. The secondary antibody mix included 5% NDS, donkey antirabbit IgG Alexa Fluor 488, and goat anti-mouse IgM Alexa Flour 657. For analysis of SERT expression, cryosections of SERT-Cre::ZsGreen brains were stained with a primary antibody mix composed of 5% NDS in  $1\times$  PBST, rabbit anti-ZsGreen, goat anti-Iba1, and mouse antineuro-filament (NF). For glia counts, Aldh1l1-eGFP mice were stained with a primary antibody mix composed of 5% NDS in  $1\times$  PBST, rabbit anti-GFP, goat anti-Iba1, and mouse anti-NF. Secondary antibody mix for

both sets of experiments was made of 5% NDS in 1X PBST, donkey anti-rabbit IgG Alexa Fluor 488, donkey anti-goat IgG Alexa Fluor 594, and donkey anti-mouse IgG 647.

### 2.3 | Imaging

All images were acquired on a Zeiss Axiolmager M2 microscope with Apotome, AxioCam MRm camera, and Neurolucida software (v11, MBF Biosciences, Williston, VT, RRID:SCR\_001775), using Fluar 5X (NA = 0.25, working distance = 12.5  $\mu$ m), Plan-APO 20X (NA = 0.8, working distance = 550  $\mu$ m), or Plan-APO 40× oil (NA = 1.4, working distance = 130  $\mu$ m) objectives. Images were acquired in MBF .tiff or .jpx format and were processed in Fiji (ImageJ, NIH, RRID:SCR\_002285).

### 2.4 | Experimental design and statistical analysis

Qualitative observations of Aldh1l1-eGFP and RC2 co-labeling were performed in one animal of each age (Figure 1a). Morphological observations of Aldh1l1+ cells and all other experiments were performed in at least five animals from 2 litters of each age (Figures 1b-6). In all experiments, male and female littermates were pooled together and analyzed as one group.

Four coronal sections through each optic tract were analyzed per mouse, within a  $20\times$  field of view for each section. The first section imaged for each set was directly caudal to the optic chiasm, with the following three the subsequent serial section proceeding caudally, at  $100 \, \mu m$  intervals. For sector analysis of SERT-Cre::ZsGreen expression,

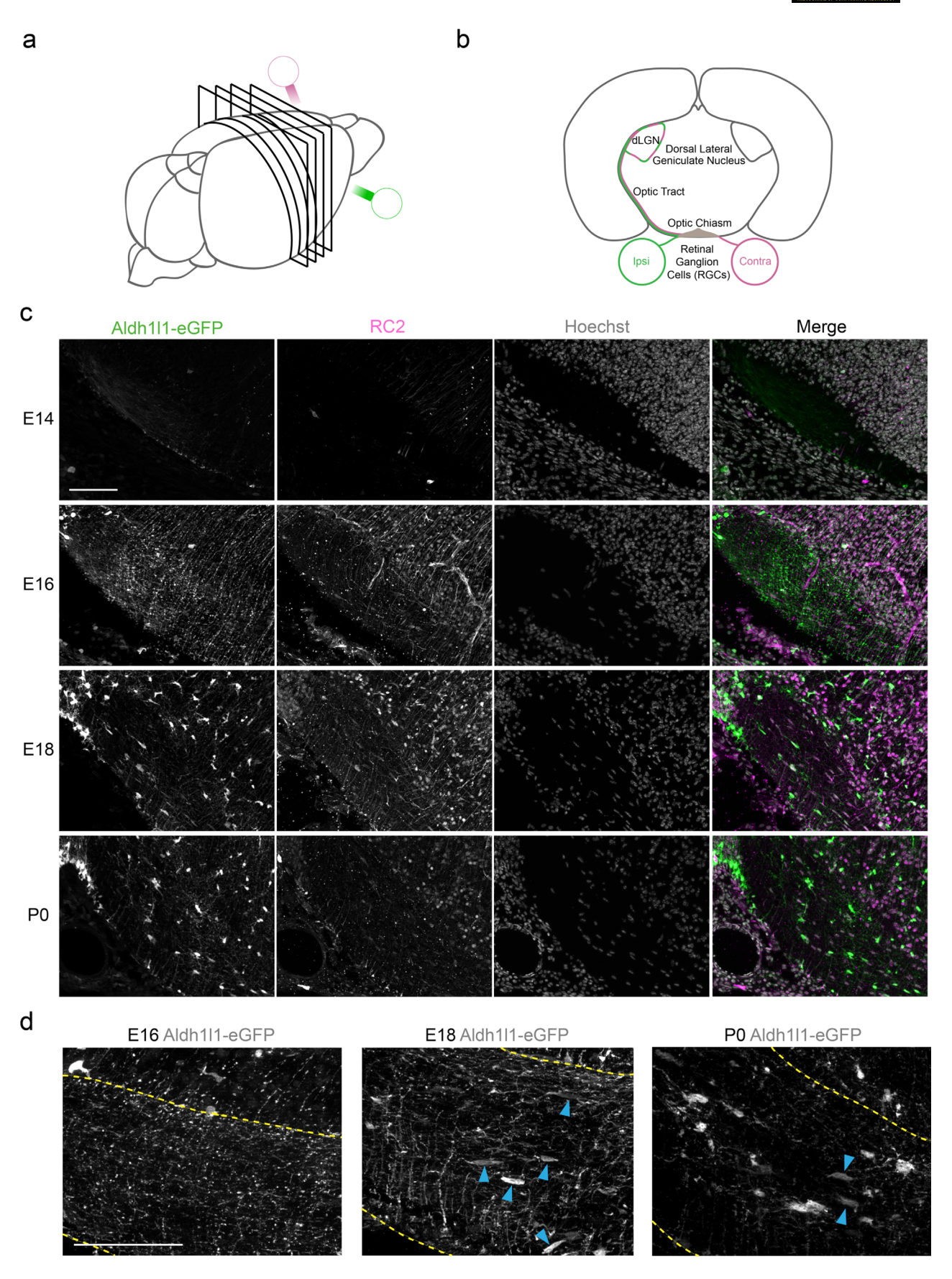


FIGURE 1 Aldh1l1-eGFP + cells include astrocytes and radial glia in the developing mouse optic tract. Frontal sections of an Aldh1l1-eGFP mouse brain taken to examine the optic tract as schematized in (a) and (b). Aldh1l1-eGFP+ labeling (green in merge) is present by E14 and is expressed almost exclusively in radial glia (magenta in merge) at E14 and E16 (c). Aldh1l1+ cell bodies appear within the optic tract by E18 and are present within the optic tract through birth. A subset of Aldh1l1+ cells (blue arrows) within the optic tract (outlined in yellow) have an elongated morphology with few processes at E18 and P0 (d). Scale bars =  $100 \mu m$ 

the optic tract was divided into three coequal sectors with a common along-tract length of 150  $\mu m,$  using the Fiji Overlay function. The width across the tract was determined at the widest point in the tract in a maximum-intensity projection of the NF signal. Using the Measure tool, the area and position of the sectors were recorded, along with the integrated density of signal within a maximum-intensity projection of the ZsGreen signal.

For analyses of glia number and distribution, the optic tract was divided into three coequal sectors as above, and two additional sectors of the same size were made directly medial and lateral to the optic tract. Cell bodies were manually counted in each optical section of a z-stack of images using Fiji based on the presence of lba1 or Aldh1l1-eGFP signal, colocalized with the Hoechst nuclear label. Graphical and statistical analyses for all experiments were performed using GraphPad Prism7 software (Version 7.0d, GraphPad Software Inc., La Jolla, CA, RRID:SCR 015807).

### 3 | RESULTS

# 3.1 | Aldh1l1+ cells are present in the optic tract and are morphologically distinct by E18

As glia provide many cues and signposts to growing axons during the development of neuronal tracts (reviewed in Learte & Hidalgo, 2007; Lemke, 2001), we specifically asked how glia are distributed in the developing optic tract relative to pre-target organization of ipsi- and contralateral RGC axons. Thus, we first set out to determine whether astrocytes are enriched in the optic tract region at early stages of retinogeniculate pathway development. Aldh1l1 is a common marker specific to astrocytes during adulthood (Cahoy et al., 2008), but is also expressed in radial glial cells during embryonic development (Molofsky et al., 2013). To distinguish between astrocytes and radial glial cells, we immunostained coronal sections through the optic tract of Aldh111eGFP mice for both GFP (to amplify the fluorescent signal of Aldh1l1+ axons) and the radial glial marker RC2 (Figure 1a,b), at four developmental time points: embryonic day (E) 14, E16, E18, and postnatal day (P) 0. At E14, the earliest-born RGC axons have navigated past the optic chiasm and the tract is predominantly composed of contralateral RGC axons, with some ipsilateral axons present as well. Both ipsi- and contralateral axons continue to grow into the tract throughout the rest of embryonic development, with most, if not all, RGC axons present in the tract by PO. Thus, the ages assessed here span an important period of retinogeniculate system development, as axons navigate through the chiasm and optic tract en route to their thalamic target, the dLGN.

GFP expression (indicating Aldh1I1+ cells and processes) was apparent at all ages examined. At E14 and E16, GFP expression was primarily radial and co-localized with RC2, with cells exclusively labeled with GFP not present until E18 (Figure 1c). Aldh1I1+ radial processes only sparsely invade the tract region at E14, but extend fairly evenly across the mediolateral width of the tract at E16. While Aldh1I1+ cell bodies were occasionally observed within the optic tract of some E16 animals, distinct Aldh1I1+ cell bodies did not consistently appear inside the tract until E18 and were not particularly abundant at any stage examined here. Notably, at E18, the Aldh1I1+ cell bodies found within the optic tract are qualitatively distinct

from those medial to the tract. Specifically, the morphology of Aldh1l1+cells within the optic tract was elongated and flattened, with few, if any, visible processes (Figure 1d, blue arrows). These oblong cells were also found sparsely within the optic tract at PO, although more complex, ramified Aldh1l1+ cells were also apparent by this age (Figure 1d).

In sum, we observe developmental changes in the presence and morphology of Aldh1I1+ cells in and around the embryonic and newborn optic tract, with radial glia processes reaching across the tract, perpendicular to growing axons, prior to E18, and more clearly delineated astrocyte cell bodies evident by E18. The distinct morphologies of astrocytes within and outside of the tract could indicate different astrocyte functions in the two regions.

## 3.2 | Ipsilateral RGCs are positioned in the lateral twothirds of the optic tract by E18

We previously reported that ipsilateral RGCs are segregated by laterality within the optic tract (Sitko et al., 2018). Here, we confirmed the lateralization of ipsilateral RGCs in the optic tract by quantifying the distribution of zsGreen signal in the SERT-Cre::zsGreen mouse across the mediolateral axis of the tract. SERT is expressed by ipsilateral, but not contralateral, RGCs in the mouse (Garcia-Frigola & Herrera, 2010; Koch et al., 2011). Here, we immunostained SERT-Cre::zsGreen brain sections for zsGreen, identifying SERT+ RGCs and their axons, and the axonal marker, NF, to identify the full width of the optic tract, at three developmental time points: E16, E18, and P0. While ipsilateral RGC axons are present in low numbers in the optic tract as early as E14, expression of zsGreen in the SERT-Cre::zsGreen mouse is not detectable prior to E16, so our analyses began at this age.

In order to quantify the extent of zsGreen fluorescence, we divided the optic tract into three coequal sectors—lateral, mid, and medial—with a fixed length of 150  $\mu m$  along the extent of the tract (Figure 2b) and measured the zsGreen integrated density (the product of the mean gray value and the area) within each sector in four serial sections along the rostrocaudal extent of the tract. The integrated density of zsGreen fluorescence intensity is relatively low and uniform across all three sectors of the optic tract at E16 (Figure 2a,c; p = .1726, one-way ANOVA). By E18, zsGreen expression is higher and is localized to the lateral and mid sectors of the tract, with fluorescence intensity highest in these two sectors relative to the medial sector (Figure 2d; p = .0007, one-way ANOVA; Lateral vs. Mid, p = .0005, Mid vs. Medial, p = .0218, Tukey's multiple comparisons test). A similar pattern also exists at PO (Figure 2e; p = .0046, one-way ANOVA; Lateral vs. Mid, p = .0040; Mid vs. Medial, p = .0428. Tukev's multiple comparisons test). These results confirm that SERT+ RGC axons are positioned with a lateral bias within the optic tract by E18 and maintain this spatial segregation after birth.

# 3.3 Aldh1l1+ cells are found within the optic tract and are transiently elevated in number medially outside of the tract

If astrocytes are involved in guiding the lateral position of ipsilateral RGC axons and/or the segregation between ipsi- and contralateral

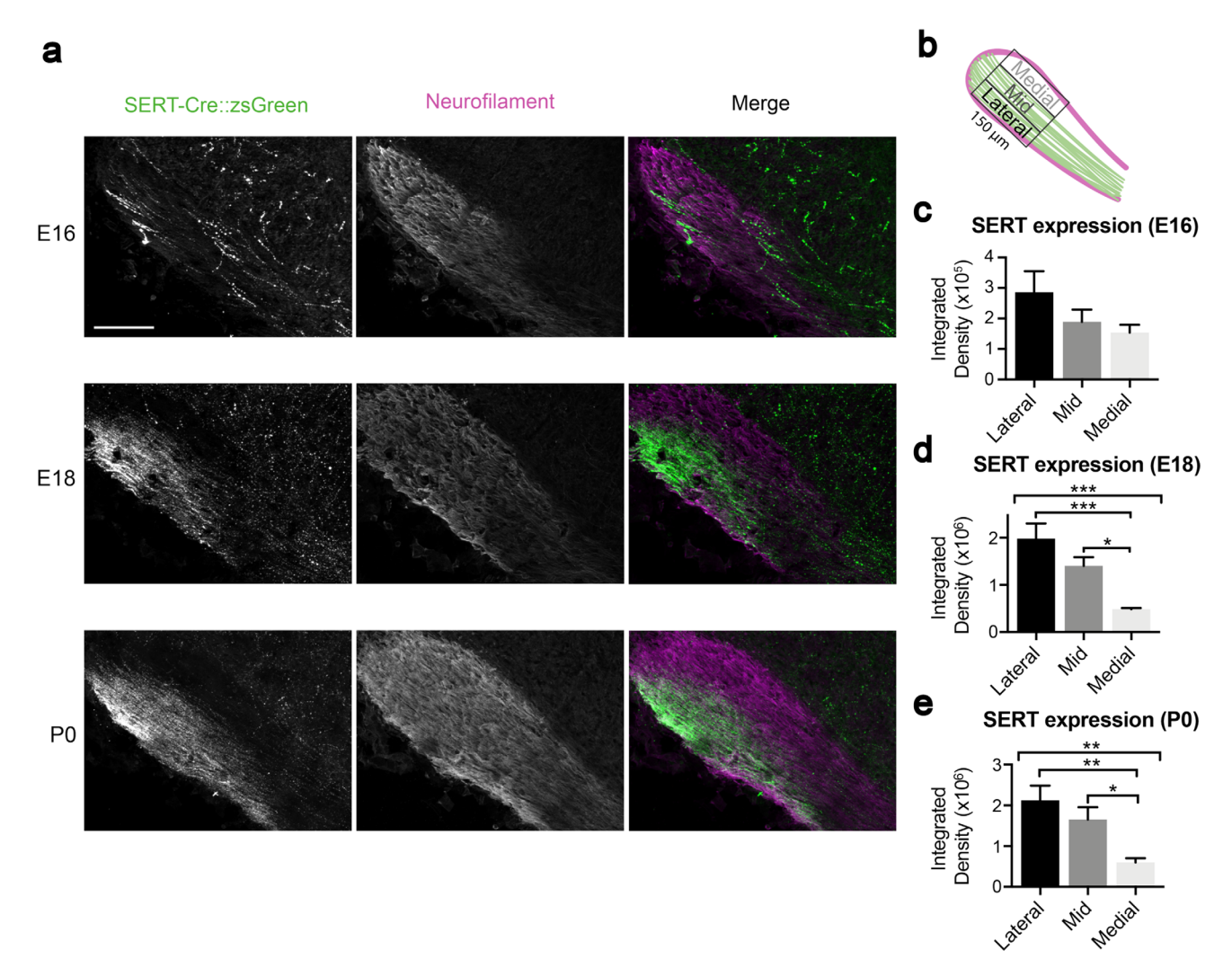


FIGURE 2 Mediolateral segregation of ipsilateral RGCs in the optic tract. SERT-Cre::zsGreen+ axons (green in merge) represent the ipsilaterally-projecting RGC axons in the optic tract (Neurofilament-positive, magenta in merge) (a) as schematized in (b). At E16, ipsilateral RGC axons are sparse and not segregated mediolaterally within the optic tract (c). By E18 and P0, ipsilateral axons are positioned in the lateral two-thirds of the optic tract (d, e). Groups were analyzed using a one-way ANOVA with Tukey's multiple corrections test (n = 5-6). p < .05 was considered statistically significant (\*p < .05, \*\*p < .01, \*\*\*p < .05). Error bars represent standard error of the mean. Scale bars = 100 µm

axons within the optic tract, then we might expect Aldh1l1+ cells to show similar spatial segregation patterns along the mediolateral aspect of the tract. To investigate this, we immunostained Aldh1I1-eGFP brain sections through the optic tract for GFP and NF at E18 and P0, the two developmental ages at which we observed Aldh1I1+ cell bodies consistently located within the tract. The tract was again divided into three coequal sectors-lateral, mid, and medial-and Aldh1l1+ cells in each sector were counted in four serial sections along the rostrocaudal length of the tract. Because we observed Aldh1I1+ cells outside of the tract (Figure 1c), we counted Aldh1l1+ cells in two additional sectors of equal width positioned on either outer side of the tract (Figure 3b). Aldh1l1+ cells were significantly elevated in number outside the medial edge of the tract at E18 (Figure 3a, c; p < .0001, one-way ANOVA; Lateral to Tract vs. Medial to Tract, p = .0014; Lateral vs. Medial to Tract, p = .0020; Mid vs. Medial to Tract, p < .0001; Medial vs. Medial to Tract, p = .0008, Tukey's multiple comparisons test).

Within the tract, there were no significant differences in number of Aldh1l1+ cells between the lateral, mid, and medial sectors at either E18 or P0. As such, the position of Aldh1l1+ cells in the tract does not mirror the lateral position of ipsilateral RGC axons. Rather, there is a preponderance of Aldh1l1+ cells in the gray matter medial to the tract.

## 3.4 | Microglia are found within the optic tract and are elevated in number lateral to the tract

We explored the possibility that microglia, which have been shown to express guidance molecules such as Plexin-A1 and Neuropilin-1 (Majed et al., 2006), may be well-positioned to guide RGC axon organization and/or eye-specific segregation within the optic tract. To do this, we immunostained Aldh1l1-eGFP mice for NF and the microglial marker lba1 and repeated the sector analysis across the mediolateral axis of the optic tract, as above. Because distinct lba+ cell bodies are present

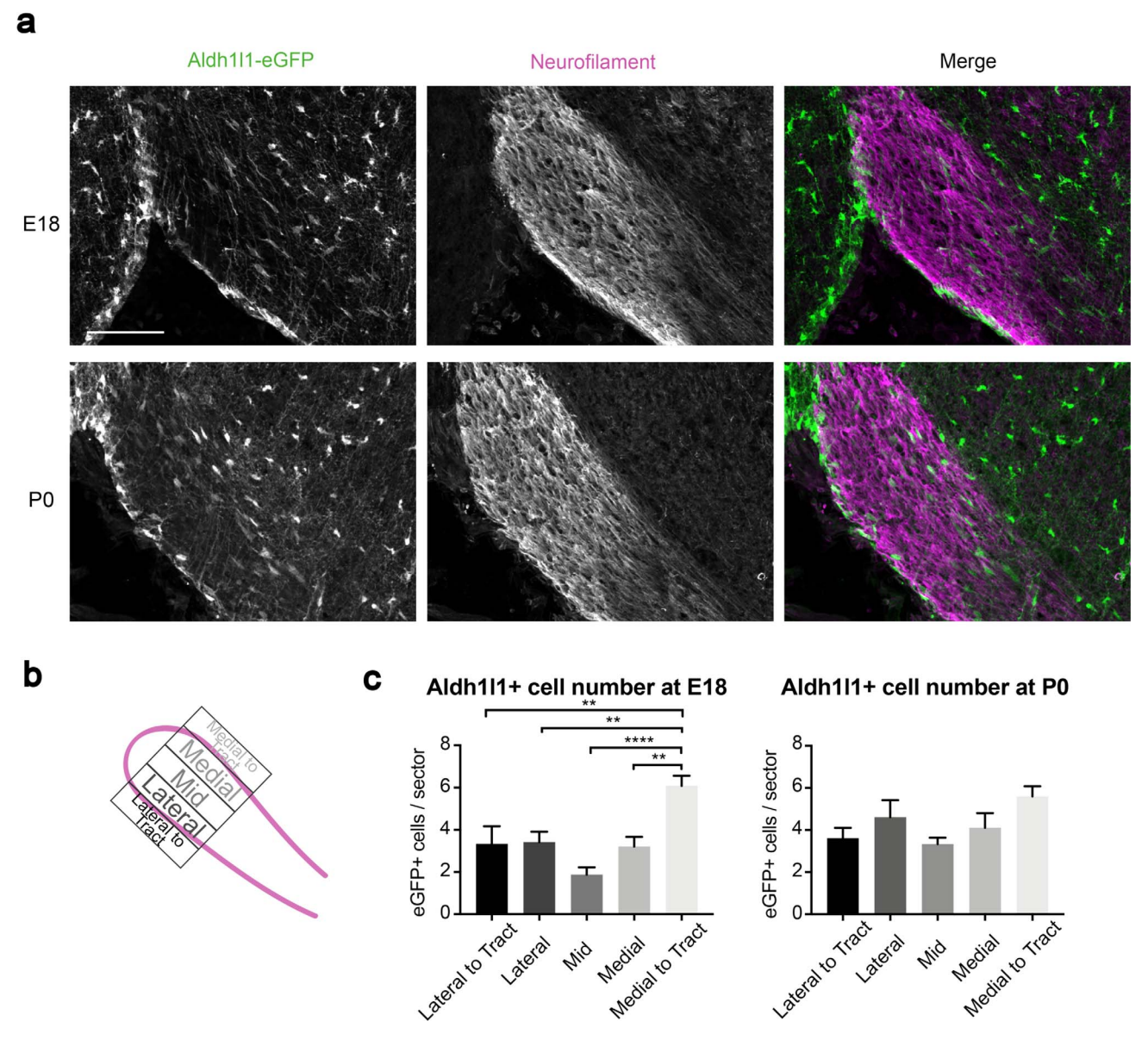


FIGURE 3 Aldh1l1+ cell numbers in and around the optic tract. Aldh1l1+ cells (green in merge) are expressed throughout and along the optic tract (magenta in merge) (a). Position of sectors analyzed is schematized in (b). Aldh1l1+ cells are elevated in number directly medial to the optic tract at E18, but not at P0 (c). Groups were analyzed using a one-way ANOVA with Tukey's multiple corrections test (n = 5-6). p < .05 was considered statistically significant (\*p < .05, \*\*p < .01, \*\*\*p < .05). Error bars represent standard error of the mean. Scale bars = 100  $\mu$ m

in the optic tract as early as E14, unlike the Aldh1l1+ signal, which remains radial until later in embryonic development, we examined four developmental time points: E14, E16, E18, and P0.

Similar to Aldh1l1+ cells, we found that microglia were few in number but present in all sectors within the optic tract at all ages examined (Figure 4a). Microglia were found in comparable numbers in all segments within the tract (Figure 4 b). They were, however, found in high numbers directly lateral to the tract (Figure 4b), where they take on a less ramified, more amoeboid shape, compared with microglia inside the tract (Figure 4a; E14, E16, E18, P0; p < .0001, one-way ANOVA; Lateral to Tract vs. Lateral, p < .0001; Lateral to Tract vs. Medial, p < .0001; Lateral to Tract vs. Medial to Tract, p < .0001, Tukey's multiple comparisons test). These

results show that, similar to astrocytes, microglia are present in and around the optic tract, but do not show expression patterns parallel to ipsilateral RGC lateralization across the mediolateral axis within the tract during late embryonic and neonatal development. Also similar to our observations of Aldh1l1+ cells, the differences in microglia morphology lateral to and within the optic tract likely indicate different functions in the two areas.

# 3.5 | Glial density within the optic tract is spatiotemporally dynamic

While our counts of Aldh1l1+ cells and microglia did not indicate a preferential localization of glia to a particular mediolateral sector of the

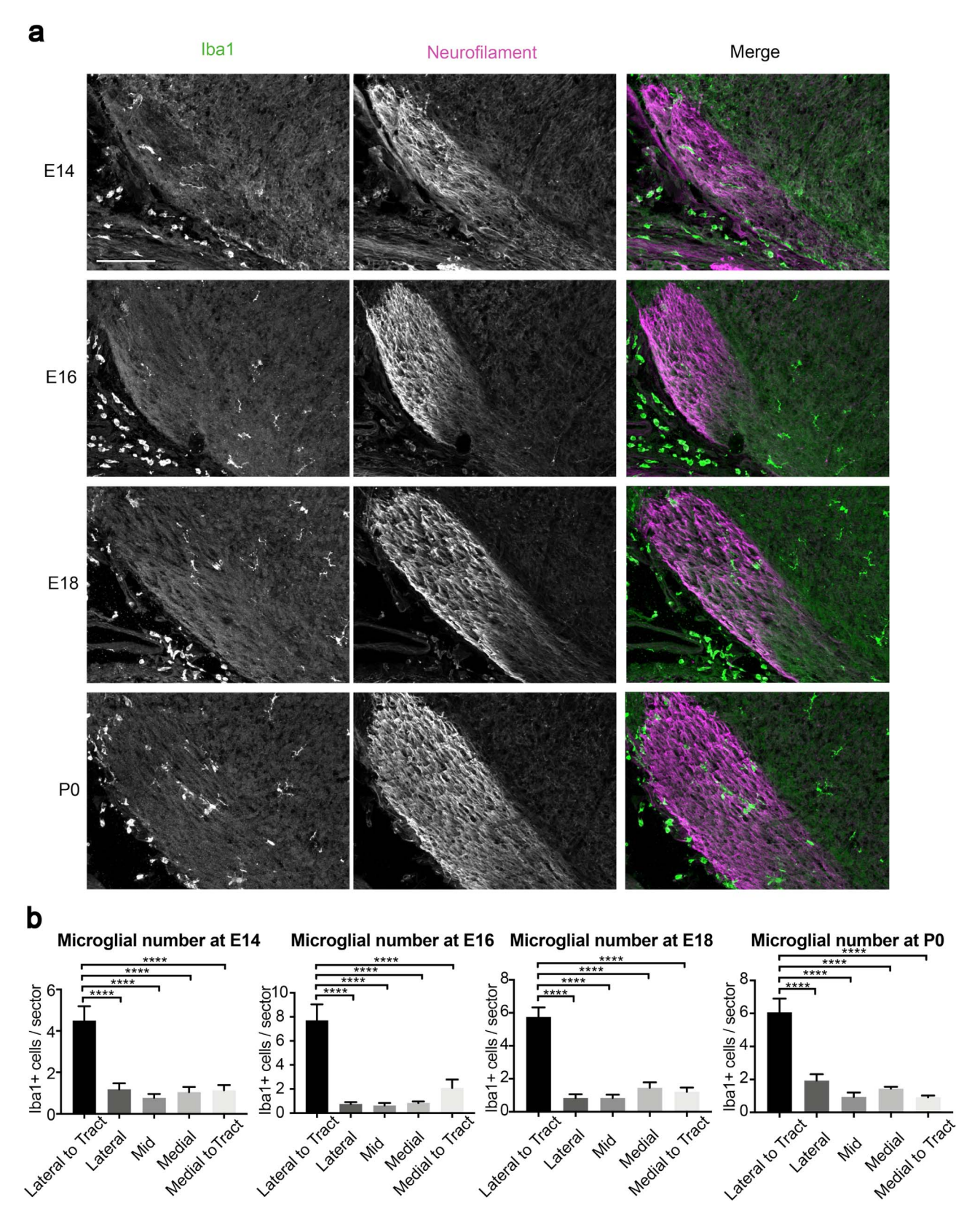


FIGURE 4 Microglia number in and around the optic tract. Microglia (green in merge) are expressed throughout and along the optic tract (magenta in merge) (a) and are elevated in number directly lateral to the optic tract at all ages examined (b). Groups were analyzed using a one-way ANOVA with Tukey's multiple corrections test (n = 5-6). p < .05 was considered statistically significant (\*p < .05, \*\*p < .01, \*\*\*p < .05). Error bars represent standard error of the mean. Scale bars = 100  $\mu$ m

optic tract, we sought to determine whether either cell type displayed subtler mediolateral distribution patterns along the length of the tract. To do this, we calculated glial density within lateral, mid, and medial sectors of the tract, using the cell counts reported above for each of the four serial sections through the tract, but taking into account tract width and area. Because the width of the optic tract varies across sections within a given animal as well as across animals, analyzing the density of Aldh1l1+ cells and microglia within each sector provides a normalized quantification of glia distribution in the tract, offering more insight than afforded by absolute cell number.

Plotting glial density within each mediolateral sector against the position of the sectors along the rostrocaudal tract length revealed significant differences in Aldh1l1+ cell density across the mediolateral axis at E18 (Figure 5a; p=.0194, two-way ANOVA). Post-hoc analysis showed that Aldh1l1+ cell density is significantly higher in the lateral sector compared to the mid sector at E18 (p=.0199, Tukey's multiple comparisons test). However, the bias of Aldh1l1+ cells toward the lateral sector of the optic tract appears to be transient—by P0, Aldh1l1+ cells are evenly distributed throughout the optic tract, with no significant differences in glial density between the lateral, mid, and medial sectors of the tract (Figure 5a).

Similarly, we identified statistically significant differences in microglia density across the mediolateral axis of the optic tract (Figure 5b) at E18 (p=.0475, two-way ANOVA) and P0 (p=.0338, two-way ANOVA), but not E14 (p=.1086, two-way ANOVA) and E16 (p=.3332, two-way ANOVA). While post-hoc analysis did not reveal any significant differences between mediolateral sector pairs at E18, microglia within the tract were higher in density in the lateral sector than in the mid sector at P0 (p=.0205, Tukey's multiple comparison test). Thus, microglia are evenly distributed throughout the mediolateral axis of the optic tract at earlier ages of development, when RGCs are initially growing into the tract, but by birth, begin to show a bias toward the lateral aspect of the optic tract.

# 3.6 | Aldh1l1+ cells, but not microglia, are biased toward the dLGN along the rostrocaudal axis of the optic tract

Using the same analysis as above, we next investigated whether glia are evenly distributed throughout the rostrocaudal extent of the optic tract, from just caudal of the optic chiasm to the dLGN. Examining Aldh1l1+ cell density across all four serial sections indicated that Aldh1l1+ cell density changes along the rostrocaudal axis of the optic tract at both E18 (p = .0122, two-way ANOVA) and P0 (p = .0109, two-way ANOVA). At both ages, Aldh1l1+ cell density increases from the anterior tract (i.e., the section just caudal to the optic chiasm) to the posterior tract (i.e., the caudal-most section, as the tract nears the dLGN) (Figure 6a). This effect appears specific to Aldh1l1+ cells, as microglia density is consistent across the rostrocaudal extent of the optic tract at each age tested (Figure 6b; E14, p = .6923; E16, p = .2926; E18, p = .8481; P0, p = .4459, two-way ANOVA). The differences in Aldh1l1+ cell and microglia distribution along the

rostrocaudal axis suggest that the two cell types may have distinct roles in optic tract development as RGC axons approach their thalamic target.

### 4 | DISCUSSION

Astrocytes are important mediators of axon guidance at choice points in developing neural circuits, such as the optic chiasm (reviewed in Herrera et al., 2017; Petros et al., 2008). Both astrocytes and microglia play a variety of roles in the developing nervous system beyond guidance at intermediate choice points (reviewed in Corty & Freeman, 2013), including axon outgrowth and laminar position of neurons (Squarzoni et al., 2014), developmental pruning and plasticity (Schafer et al., 2012), and fasciculation and organization of axons (Pont-Lezica et al., 2014). In the visual system, changes in glial morphology and orientation from the nerve to the chiasm have been suggested to play a role in establishing topographic (e.g., Reese et al., 1994) or age-related order (e.g., Maggs & Scholes, 1986; Reese et al., 1997) of growing RGC axons, but this has not been fully investigated, and glia in the mouse optic tract in particular remain poorly understood.

We aimed here to assess features of two types of glia-presumptive astrocytes (using genetic labeling of Aldh1l1) and microglia (using immunohistochemical labeling of Iba1)-in and around the developing optic tract, as they relate to ipsilateral RGC axon position in the lateral aspect of the tract and segregation of ipsi- and contralateral RGC axons. Specifically, we examined the numbers and distribution of astrocytes and microglia along the mediolateral and rostrocaudal axes of the tract, assessing whether and how glial morphology and distribution change over the course of tract development, from early axon growth into the tract at E14 through birth, when pre-target axon organization has been established within the optic tract. While we found that glial positioning did not parallel the mediolateral segregation of eye-specific RGC axons, we observed distinct spatiotemporal organizational patterns in the distribution of Aldh1l1-expressing astrocytes and Iba1expressing microglia, expanding our understanding of the distribution of these cells relative to the growing retinogeniculate axon tract during a significant developmental period.

Aldh1l1+ cells and microglia are present in comparable numbers in the lateral-most two-thirds of the optic tract, where ipsilateral axons reside (see Figure 2 and Sitko et al., 2018), and in the medial third of the tract, where contralateral axons predominate. The relatively uniform number of both Aldh1l1+ cells and microglia in each of the sectors across the mediolateral axis of the optic tract is consistent across all developmental ages examined. However, analyzing the density of glia along both the mediolateral and rostrocaudal axes provided more insight into the overall distribution of astrocytes and microglia in the developing tract. Namely, Aldh1l1+ cells are transiently biased toward the lateral tract and are consistently distributed closer to the dLGN along the rostrocaudal axis, while microglia display no rostrocaudal distribution patterns during development but are preferentially distributed to the lateral tract at birth (Figures 5 and 6). Additionally, there is a preponderance of Aldh1l1+ cells and microglia outside of the tract,

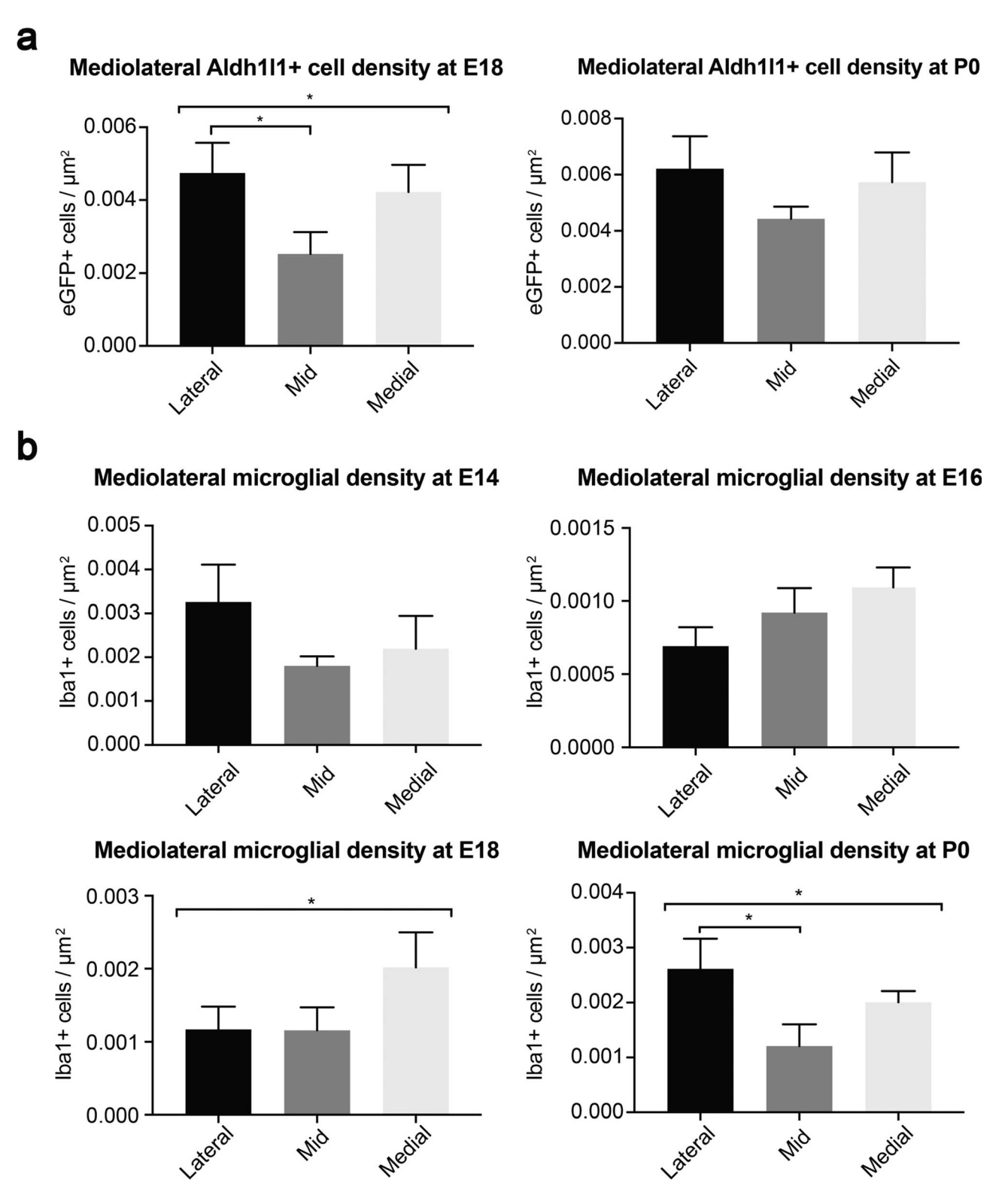


FIGURE 5 Aldh1l1+ cell and microglia density in the mediolateral dimension within the optic tract. Aldh1l1+ cell density is higher in the lateral-most sector within the optic tract at E18, but not P0 (a). Microglia density is consistent throughout the optic tract at earlier ages, E14 and E16 (b). By E18, however, microglia density is higher in the lateral-most sector of the optic tract, a pattern that is maintained through birth. Groups were analyzed using a one-way ANOVA with Tukey's multiple corrections test (n = 5-6). p < .05 was considered statistically significant (\*p < .05, \*\*p < .01, \*\*\*p < .05). Error bars represent standard error of the mean

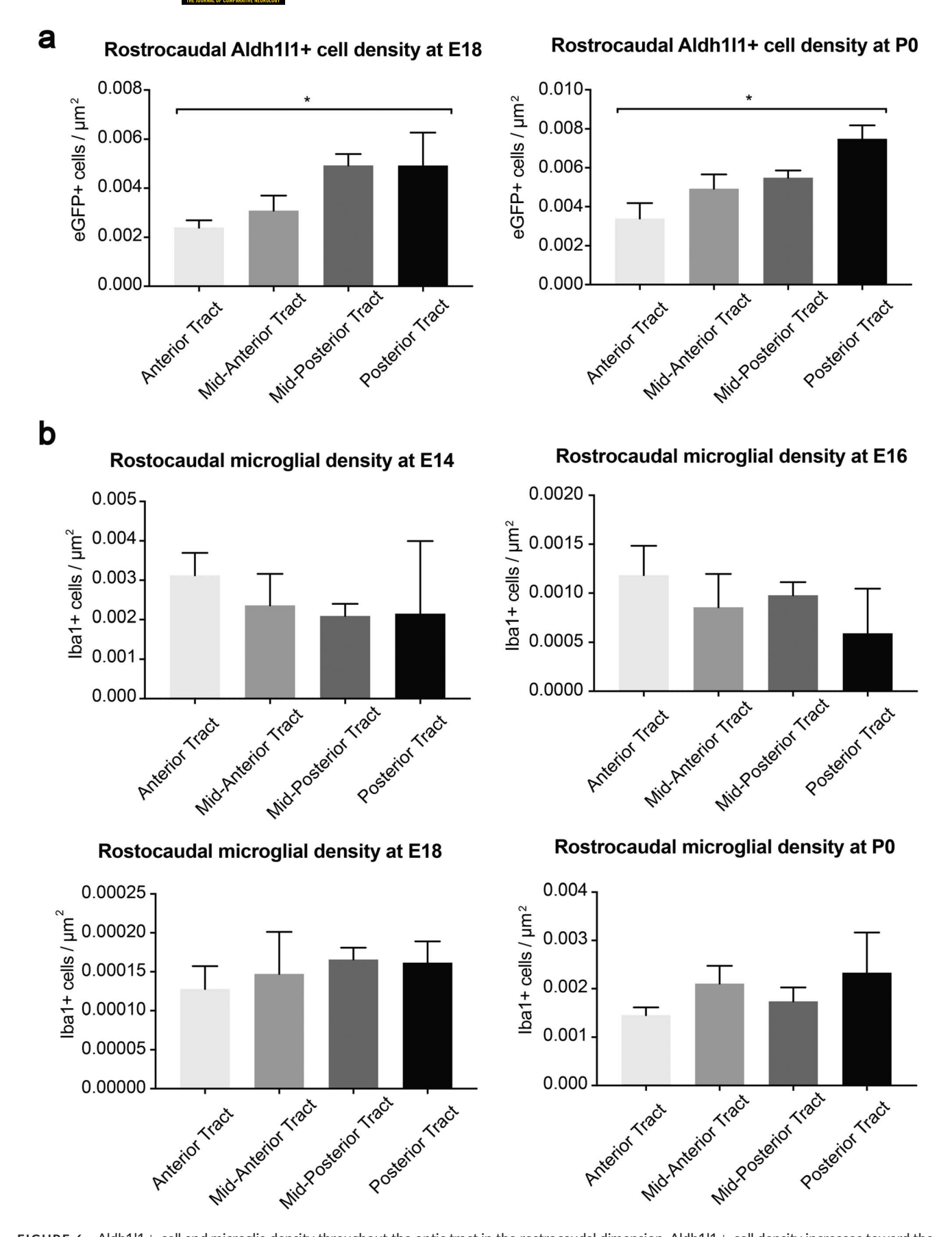


FIGURE 6 Aldh1l1+ cell and microglia density throughout the optic tract in the rostrocaudal dimension. Aldh1l1+ cell density increases toward the caudal aspect in the posterior sections of the optic tract at both E18 and P0 (a). In contrast, microglia density is consistent throughout the optic tract in the rostrocaudal dimension at all ages examined (b). Groups were analyzed using a one-way ANOVA with Tukey's multiple corrections test (n = 5-6). p < .05 was considered statistically significant (\*p < .05, \*\*p < .05). Error bars represent standard error of the mean

519

medially and laterally, respectively, throughout embryonic and neonatal optic tract development (Figures 3c and 4b).

The distribution patterns of the glia presented here do not directly implicate either class of cells in mediating ipsilateral RGC axon position to the lateral tract or the segregation between ipsilateral and contralateral axons previously reported (Sitko et al., 2018). However, the subtle bias of both Aldh1l1+ cells and microglia toward to the lateral segment of the tract at the end of embryonic development (Figure 5) is suggestive of a possible role in the lateral position of ipsilateral retinal axons. Even in the absence of direct spatial relationships between ipsilateral RGC axons and astrocytes or microglia, however, glia may well contribute to eye-specific segregation of RGC axons en route to the dLGN and SC by presenting molecular cues specific to ipsi- and contralateral RGC axons. One limitation of our study is that by using Aldh1I1 and Iba1 as markers of astrocytes and microglia, respectively, we are blind to the molecular heterogeneity within either population of cells. Both astrocytes and microglia are highly heterogeneous groups of cells with subpopulations engaging in a variety of specific roles, the details of which are still being actively explored (Chai et al., 2017; Grabert et al., 2016). Indeed, we observed two distinct populations of Aldh1l1+ cells in the optic tract-those colocalized with RC2 and those expressing Aldh111-eGFP alone. Future studies could utilize additional known glial markers, including GFAP, Vimentin, Aquaporin-4, and S100B, to identify specific subsets of astrocytes relative to RGC axon cohorts. Single cell RNA sequencing of putative astrocytes isolated from the optic tracts of Aldh1I1-eGFP mice could provide even more insight into the heterogeneity of optic tract astrocytes in the future. Sequencing experiments would likely reveal novel markers for subsets of astrocytes in the tract, which histological analyses could then relate to ipsilateral and contralateral RGC axon cohorts.

Aldh1l1+ cell density increases with proximity to the dLGN along the rostrocaudal axis of the optic tract at both E18 and P0 (Figure 6). This is in contrast with microglia, which are evenly distributed along the rostrocaudal axis of the optic tract at all ages examined, suggesting that the two cell types are functionally divergent in tract development. One possible explanation for the increase in rostrocaudal density of Aldh1l1+ cells near the dLGN is that the flattened, elongated Aldh1l1+ cells we observe may be migrating along the optic tract toward the target. It is also possible that, along the lines of Vivien Casagrade's findings (Hutchins & Casagrande, 1988, 1990), Aldh1l1+ cells act as mediators of early targeting to the dLGN, guiding axons as they exit the tract to enter the target. These two explanations are not mutually exclusive, and further study will be required to elucidate the significance of increasing astrocyte density as RGC axons approach the dLGN.

Embryonic day 18 emerges as an important developmental time point in our analyses. Specifically, coincident with ipsilateral RGCs segregating into the lateral two-thirds of the optic tract (see Figure 2 and Sitko et al., 2018), distinct flattened, elongated Aldh1l1+ cells appear in the tract and are temporarily biased toward the lateral-most sector of the tract. Outside of the tract, Aldh1l1+ cells are higher in number directly medial to the tract at E18, a pattern that is also no longer present by P0 (Figure 3c). Microglia, which are evenly distributed across

the mediolateral axis of the tract at E14 and E16, also become lateralized at E18 (Figure 4b). In contrast with Aldh1l1+ cells, however, microglial lateralization persists through birth. The concurrence of these features of glial distribution with the emergence of clear ipsilateral segregation to the lateral optic tract suggests a potential relationship between glia and axon position. Understanding the molecular profiles of both glia and eye-specific cohorts of retinal axons in the tract will help elucidate whether such a relationship exists, what the nature of that relationship might be, and how it may contribute to the development of the retinogeniculate circuit.

Glia are located in relatively high numbers directly outside of the optic tract at all ages examined, as compared with glia number within the tract. Curiously, while this is true for both cell types we examined, Aldh1l1+ cells are primarily located on the outer medial edge of the tract along the gray matter, while microglia are primarily located on the outer lateral aspect of the tract, along and outside of the glia limitans. The microglia lateral to the tract are amoeboid in morphology, rather than the ramified microglia seen inside the optic tract. How these morphological differences might influence their relationship with and possible effects on retinal axons in the optic tract is unclear.

Appreciation of cellular morphology and organization in developing tissues has a rich history in neurobiology, reaching back to seminal work by Santiago Ramón y Cajal, and anatomical approaches have helped elucidate many novel and important principles of neural development (Godement, Salaun, & Mason, 1990; Guillery & Walsh, 1987; Hutchins & Casagrande, 1988). The qualitative and quantitative account of the distribution of glia cells presented here builds on this legacy and furthers our understanding of the spatiotemporal dynamics of astrocytes and microglia in the embryonic and neonatal mouse optic tract. This knowledge provides a necessary foundation for probing the molecular mechanisms of glial contributions to axon growth and organization within the developing tract in the future.

#### **ACKNOWLEDGMENTS**

This work was supported by NIH Grants R01 EY012736, R01 GM105775, and T32 EY013933. H. Melikyan provided technical assistance with mouse husbandry and J. Peregrin assisted with histology preparation. We thank members of the Mason and Dodd Labs for feedback and suggestions.

### **CONFLICT OF INTEREST**

The authors declare no competing financial interests.

## ORCID

Melissa A. Lee http://orcid.org/0000-0003-4965-1536

Austen A. Sitko http://orcid.org/0000-0002-7601-6143

Mimi Shirasu-Hiza http://orcid.org/0000-0002-2730-1765

Carol A. Mason http://orcid.org/0000-0001-6253-505X

### **REFERENCES**

- Barres, B. A., & Barde, Y. (2000). Neuronal and glial cell biology. Current Opinion in Neurology, 10(5), 642–648.
- Bovolenta, P., & Mason, C. (1987). Growth cone morphology varies with position in the developing mouse visual pathway from retina to first targets. *Journal of Neuroscience*, 7(5), 1447–1460.
- Cahoy, J. D., Emery, B., Kaushal, A., Foo, L. C., Zamanian, J. L., Christopherson, K. S., ... Barres, B. A. (2008). A transcriptome database for astrocytes, neurons, and oligodendrocytes: a new resource for understanding brain development and function. *Journal of Neuroscience*, 28 (1), 264–278. https://doi.org/10.1523/JNEUROSCI.4178-07.2008
- Chai, H., Diaz-Castro, B., Shigetomi, E., Monte, E., Octeau, J. C., Yu, X., ... Khakh, B. S. (2017). Neural circuit-specialized astrocytes: Transcriptomic, proteomic, morphological, and functional evidence. *Neuron*, 95(3), 531–549. e539. https://doi.org/ 10.1016/j.neuron.2017.06.029
- Chan, S. O., & Chung, K. Y. (1999). Changes in axon arrangement in the retinofugal [correction of retinofungal] pathway of mouse embryos: Confocal microscopy study using single- and double-dye label. *Journal* of Comparative Neurology, 406(2), 251–262.
- Chung, W. S., Clarke, L. E., Wang, G. X., Stafford, B. K., Sher, A., Chakraborty, C., ... Barres, B. A. (2013). Astrocytes mediate synapse elimination through MEGF10 and MERTK pathways. *Nature*, 504(7480), 394–400. https://doi.org/10.1038/nature12776
- Clarke, L. E., & Barres, B. A. (2013). Emerging roles of astrocytes in neural circuit development. *Nature Reviews Neuroscience*, 14(5), 311–321. https://doi.org/ 10.1038/nrn3484
- Colello, R. J., & Guillery, R. W. (1992). Observations on the early development of the optic nerve and tract of the mouse. *Journal of Comparative Neurology*, 317(4), 357–378. https://doi.org/ 10.1002/cne.903170404
- Corty, M. M., & Freeman, M. R. (2013). Cell biology in neuroscience: Architects in neural circuit design: glia control neuron numbers and connectivity. *Journal of Cell Biology*, 203(3), 395–405. https://doi.org/ 10.1083/jcb.201306099
- Garcia-Frigola, C., & Herrera, E. (2010). Zic2 regulates the expression of SERT to modulate eye-specific refinement at the visual targets. *The EMBO Journal*, 29(18), 3170–3183. https://doi.org/10.1038/emboj. 2010.172
- Godement, P., Salaun, J., & Imbert, M. (1984). Prenatal and postnatal development of retinogeniculate and retinocollicular projections in the mouse. *Journal of Comparative Neurology*, 230(4), 552–575. https://doi.org/10.1002/cne.902300406
- Godement, P., Salaun, J., & Mason, C. A. (1990). Retinal axon pathfinding in the optic chiasm: Divergence of crossed and uncrossed fibers. *Neuron*, 5(2), 173–186.
- Godement, P., Wang, L. C., & Mason, C. A. (1994). Retinal axon divergence in the optic chiasm: Dynamics of growth cone behavior at the midline. *Journal of Neuroscience*, 14(11 Pt 2), 7024–7039.
- Gong, S., Doughty, M., Harbaugh, C. R., Cummins, A., Hatten, M. E., Heintz, N., & Gerfen, C. R. (2007). Targeting Cre recombinase to specific neuron populations with bacterial artificial chromosome constructs. J Neurosci, 27(37), 9817–9823. https://doi.org/10.1523/ JNEUROSCI.2707-07.2007
- Grabert, K., Michoel, T., Karavolos, M. H., Clohisey, S., Baillie, J. K., Stevens, M. P., . . . McColl, B. W. (2016). Microglial brain region-dependent diversity and selective regional sensitivities to aging. *Nature Neuroscience*, 19 (3), 504–516. https://doi.org/10.1038/nn.4222
- Guillery, R. W., & Walsh, C. (1987). Changing glial organization relates to changing fiber order in the developing optic nerve of ferrets. *Journal*

- of Comparative Neurology, 265(2), 203-217. https://doi.org/10.1002/cne.902650205
- Herrera, E., Erskine, L., & Morenilla-Palao, C. (2017). Guidance of retinal axons in mammals. Seminars in Cell and Developmental Biology, https://doi.org/10.1016/j.semcdb.2017.11.027
- Hutchins, J. B., & Casagrande, V. A. (1988). Glial cells develop a laminar pattern before neuronal cells in the lateral geniculate nucleus. Proceedings of the National Academy of Sciences of the United States of America, 85(21), 8316–8320.
- Hutchins, J. B., & Casagrande, V. A. (1989). Vimentin: changes in distribution during brain development. Glia, 2(1), 55–66. https://doi.org/10.1002/glia.440020107
- Hutchins, J. B., & Casagrande, V. A. (1990). Development of the lateral geniculate nucleus: Interactions between retinal afferent, cytoarchitectonic, and glial cell process lamination in ferrets and tree shrews. *Journal of Comparative Neurology*, 298(1), 113–128. https://doi.org/ 10.1002/cne.902980109
- Imai, T., Yamazaki, T., Kobayakawa, R., Kobayakawa, K., Abe, T., Suzuki, M., & Sakano, H. (2009). Pre-target axon sorting establishes the neural map topography. *Science*, 325(5940), 585–590. https://doi.org/10.1126/science.1173596
- Inoue, Y. (1970). The glioarchitectonics of the chicken brain. I. The glial cells in the optic tract. *Okajimas Folia Anatomica Japonica*, 47(4), 229–265.
- Koch, S. M., Dela Cruz, C. G., Hnasko, T. S., Edwards, R. H., Huberman, A. D., & Ullian, E. M. (2011). Pathway-specific genetic attenuation of glutamate release alters select features of competition-based visual circuit refinement. *Neuron*, 71(2), 235–242. https://doi.org/10.1016/ j.neuron.2011.05.045
- Kuwajima, T., Yoshida, Y., Takegahara, N., Petros, T., Kumanogoh, A., Jessell, T. M., ... Mason, C. A. (2012). Optic chiasm presentation of semaphorin6D in the context of plexin-A1 and Nr-CAM promotes retinal axon midline crossing. *Neuron*, 74(4), 676–690. http://doi.org/10.1016/j.neuron.2012.03.025
- Learte, A. R., & Hidalgo, A. (2007). The role of glial cells in axon guidance, fasciculation and targeting. Advances in Experimental Medicine and Biology, 621, 156–166. http://doi.org/10.1007/978-0-387-76715-4 12
- Lemke, G. (2001). Glial control of neuronal development. Annual Review of Neuroscience, 24, 87–105. http://doi.org/10.1146/annurev.neuro. 24.1.87
- Levine, R. L. (1989). Organization of astrocytes in the visual pathways of the goldfish: An immunohistochemical study. *Journal of Comparative Neurology*, 285(2), 231–245. http://doi.org/10.1002/cne.902850206
- Maggs, A., & Scholes, J. (1986). Glial domains and nerve fiber patterns in the fish retinotectal pathway. The Journal of Neuroscience, 6(2), 424– 438.
- Majed, H. H., Chandran, S., Niclou, S. P., Nicholas, R. S., Wilkins, A., Wing, M. G., . . . Compston, A. (2006). A novel role for Sema3A in neuroprotection from injury mediated by activated microglia. *The Journal of Neuroscience*, 26(6), 1730–1738. http://doi.org/10.1523/JNEUROSCI.0702-05.2006
- Mason, C. A., & Sretavan, D. W. (1997). Glia, neurons, and axon pathfinding during optic chiasm development. *Current Opinion in Neurobiology*, 7(5), 647–653.
- Mason, C. A., & Wang, L. C. (1997). Growth cone form is behaviorspecific and, consequently, position-specific along the retinal axon pathway. *Journal of Neuroscience*, 17(3), 1086–1100.
- Molofsky, A. V., Glasgow, S. M., Chaboub, L. S., Tsai, H. H., Murnen, A. T., Kelley, K. W., ... Oldham, M. C. (2013). Expression profiling of

521

- Aldh1l1-precursors in the developing spinal cord reveals glial lineage-specific genes and direct Sox9-Nfe2l1 interactions. *Glia*, 61(9), 1518–1532. https://doi.org/10.1002/glia.22538
- Petros, T. J., Rebsam, A., & Mason, C. A. (2008). Retinal axon growth at the optic chiasm: to cross or not to cross. *Annual Review of Neuroscience*, 31, 295–315. https://doi.org/10.1146/annurev.neuro.31. 060407.125609
- Pont-Lezica, L., Beumer, W., Colasse, S., Drexhage, H., Versnel, M., & Bessis, A. (2014). Microglia shape corpus callosum axon tract fasciculation: Functional impact of prenatal inflammation. *European Journal of Neuroscience*, 39(10), 1551–1557. https://doi.org/10.1111/ejn.12508
- Reese, B. E., Johnson, P. T., Hocking, D. R., & Bolles, A. B. (1997). Chronotopic fiber reordering and the distribution of cell adhesion and extracellular matrix molecules in the optic pathway of fetal ferrets. *Journal of Comparative Neurology*, 380(3), 355–372.
- Reese, B. E., Maynard, T. M., & Hocking, D. R. (1994). Glial domains and axonal reordering in the chiasmatic region of the developing ferret. *Journal of Comparative Neurology*, 349(2), 303–324. https://doi.org/ 10.1002/cne.903490211
- Schafer, D. P., Lehrman, E. K., Kautzman, A. G., Koyama, R., Mardinly, A. R., Yamasaki, R., . . . Stevens, B. (2012). Microglia sculpt postnatal neural circuits in an activity and complement-dependent manner. *Neuron*, 74 (4), 691–705. http://doi.org/10.1016/j.neuron.2012.03.026
- Sitko, A. A., Kuwajima, T., & Mason, C. A. (2018). Eye-specific segregation and differential fasciculation of developing retinal ganglion cell axons in the mouse visual pathway. *Journal of Comparative Neurology*, http://doi.org/10.1002/cne.24392
- Squarzoni, P., Oller, G., Hoeffel, G., Pont-Lezica, L., Rostaing, P., Low, D., ... Garel, S. (2014). Microglia modulate wiring of the embryonic forebrain. *Cell Reports*, 8(5), 1271–1279. http://doi.org/10.1016/j.celrep. 2014.07.042

- Stogsdill, J. A., & Eroglu, C. (2017). The interplay between neurons and glia in synapse development and plasticity. *Current Opinion in Neurology*, 42, 1–8. http://doi.org/10.1016/j.conb.2016.09.016
- Vanselow, J., Thanos, S., Godement, P., Henke-Fahle, S., & Bonhoeffer, F. (1989). Spatial arrangement of radial glia and ingrowing retinal axons in the chick optic tectum during development. Brain Research. Developmental Brain Research, 45(1), 15–27.
- Wang, L., Mongera, A., Bonanomi, D., Cyganek, L., Pfaff, S. L., Nusslein-Volhard, C., & Marquardt, T. (2014). A conserved axon type hierarchy governing peripheral nerve assembly. *Development*, 141(9), 1875–1883. http://doi.org/10.1242/dev.106211
- Williams, R. W., & Rakic, P. (1985). Dispersion of growing axons within the optic nerve of the embryonic monkey. Proceedings of the National Academy of Sciences of the United States of America, 82(11), 3906– 3910.
- Williams, S. E., Mann, F., Erskine, L., Sakurai, T., Wei, S., Rossi, D. J., ... Henkemeyer, M. (2003). Ephrin-B2 and EphB1 mediate retinal axon divergence at the optic chiasm. *Neuron*, 39(6), 919–935.
- Zhou, J., Wen, Y., She, L., Sui, Y. N., Liu, L., Richards, L. J., & Poo, M. M. (2013). Axon position within the corpus callosum determines contralateral cortical projection. *Proceedings of the National Academy of Sciences of the United States of America*, 110(29), E2714–E2723. http://doi.org/10.1073/pnas.1310233110

How to cite this article: Lee MA, Sitko AA, Khalid S, MShirasu-Hiza, Mason CA. Spatiotemporal distribution of glia in and around the developing mouse optic tract.. *J Comp Neurol.* 2019;527:508–521. https://doi.org/10.1002/cne.24462